



# Iridium-Catalyzed Reductive Carbon–Carbon Bond Cleavage Reaction on a Curved Pyridylcorannulene Skeleton\*\*

Shohei Tashiro, Mihoko Yamada, and Mitsuhiro Shionoya\*

**Abstract:** The cleavage of C–C bonds in  $\pi$ -conjugated systems is an important method for controlling their shape and coplanarity. An efficient way for the cleavage of an aromatic C–C bond in a typical buckybowl corannulene skeleton is reported. The reaction of 2-pyridylcorannulene with a catalytic amount of  $\text{IrCl}_3 \cdot n\text{H}_2\text{O}$  in ethylene glycol at 250 °C resulted in a structural transformation from the curved corannulene skeleton to a strain-free flat benzo[ghi]fluoranthene skeleton through a site-selective C–C cleavage reaction. This cleavage reaction was found to be driven by both the coordination of the 2-pyridyl substituent to iridium and the relief of strain in the curved corannulene skeleton. This finding should facilitate the design of carbon nanomaterials based on C–C bond cleavage reactions.

Carbon nanomaterials, such as fullerenes, carbon nanotubes, graphene, carbon nanorings, and buckybawls, are organic materials that have recently attracted increasing attention,<sup>[1]</sup> and the chemical modification of their basic skeletons is essential to expand the capability of such materials. The most typical transformations entail structural extension by attaching functionality.<sup>[1,2]</sup> On the other hand, cutting the carbon nanomaterials through C–C bond cleavage has also been developed as a unique and useful transformation to obtain hard-to-find structures.<sup>[3]</sup> For example, fullerenes were holed to encapsulate guest species.<sup>[3c]</sup> Carbon nanotubes have also been cleaved to open the nanotube termini<sup>[3e]</sup> or to shorten the nanotubes.<sup>[3f]</sup> Another remarkable example is the unzipping of carbon nanotubes<sup>[3g]</sup> and graphene sheets<sup>[3h]</sup> through successive C–C bond cleavage reactions.

Corannulene<sup>[4a]</sup> is a typical buckybowl,<sup>[4]</sup> and its characteristic properties, which result from the curved structure, such as bowl-to-bowl inversion,<sup>[5a,b]</sup> molecular recognition,<sup>[5c,d]</sup> metal complexation,<sup>[5e,f]</sup> and self-association,<sup>[5g,h]</sup> have attracted much attention. As with other carbon nanomaterials, there are many reports of the structural extension of the corannulene skeleton through modifications of its periphery.<sup>[1e,5c,g,h,6]</sup> In contrast, C–C bond cleavage reactions of less

strained buckybowl skeletons are limited to only a few special examples, such as the fragmentation of corannulene during mass measurements, the cleavage of a strongly distorted corannulene derivative during flash vacuum pyrolysis, the ring opening of decapentynylcorannulene via a diradical intermediate, and laser annealing or oxone oxidation of sumanene derivatives.<sup>[7]</sup> Herein, we report an efficient and selective C–C bond cleavage reaction of a curved corannulene skeleton by using  $\text{IrCl}_3 \cdot n\text{H}_2\text{O}$  as a catalyst under microwave heating at 250 °C in ethylene glycol to obtain a flat benzo[ghi]fluoranthene skeleton (Figure 1). It was suggested that relief of the nonplanar strain in the corannulene skeleton was an important factor contributing to the

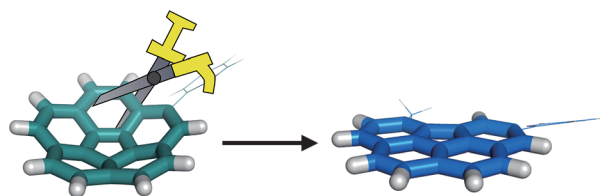


**Figure 1.** C–C bond cleavage and concomitant planarization of a corannulene skeleton.

cleavage through insertion of iridium into the C–C bond. C–C bond activation of strained compounds with transition metals is a hot topic in this field,<sup>[8]</sup> and for example, oxidative addition reactions of metals to strongly distorted carbon nanomaterials, such as deeper buckybawls and open-cage fullerenes have been reported, but the inserted metals were still present in the products.<sup>[9]</sup> However, to the best of our knowledge, catalytic bond cleavage reactions of less distorted corannulenes<sup>[10]</sup> with metals have not been reported. Indeed, it was found that among the late transition metals commonly employed, this reaction was specific to iridium.

We have previously reported that 2-pyridylcorannulene (**1**) reacted with a  $\text{Pd}^{\text{II}}$  salt to form the cyclopalladated complex  $[\text{Pd}(\text{1-H})(\text{CH}_3\text{CN})_2]\text{BF}_4$  under mild conditions (60 °C).<sup>[11]</sup> In the current study, it was found that the corannulene skeleton of **1** was readily cleaved by a catalytic amount of  $\text{IrCl}_3 \cdot n\text{H}_2\text{O}$  (0.1 equiv) under microwave heating (250 °C) for 30 minutes (Figure 2a). The resulting yellow suspension that contained some metallic solid was initially purified by extraction with  $\text{CH}_2\text{Cl}_2$  to obtain a crude product.  $^1\text{H}$  NMR spectroscopy of the crude product indicated that the starting material **1** had been completely consumed, and that a new species had been generated instead (Figure 2b,c). After further purification, the product of C–C bond cleavage, 2-(6-ethylbenzo[ghi]fluoranthene-4-yl)pyridine (**2**), was iso-

[\*] Dr. S. Tashiro, Dr. M. Yamada, Prof. Dr. M. Shionoya  
Department of Chemistry, Graduate School of Science  
The University of Tokyo  
7-3-1 Hongo, Bunkyo-ku, Tokyo 113-0033 (Japan)  
E-mail: shionoya@chem.s.u-tokyo.ac.jp

[\*\*] This study was supported by the JSPS (KAKENHI Grant 26248016 to M.S.) and the “Nanotechnology Platform” (12024046) of MEXT (Japan). M.Y. thanks the JSPS for a JSPS Research Fellowship for Young Scientists.

Supporting information for this article is available on the WWW under <http://dx.doi.org/10.1002/anie.201500819>.

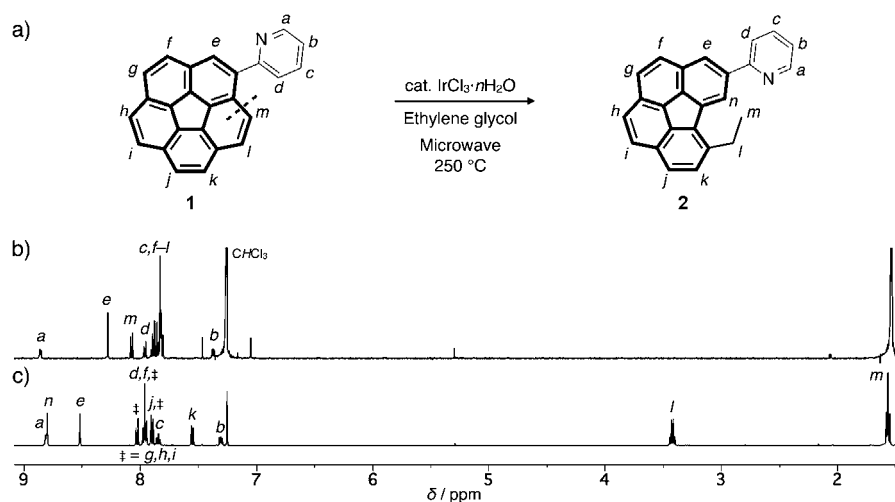


**Figure 2.** a) Reaction conditions of the iridium-catalyzed conversion of **1** into **2**. b, c)  $^1\text{H}$  NMR spectra (500 MHz,  $\text{CDCl}_3$ , 300 K) of **1** (b) and **2** (c).

lated in 87% yield as a yellow solid. The  $^1\text{H}$  NMR spectrum of **2** in  $\text{CDCl}_3$  gave two signals characteristic of an ethyl moiety in the aliphatic region at 3.42 and 1.57 ppm. The number of  $^1\text{H}$  NMR signals in the aromatic region also decreased to twelve protons. These results suggested that one of the C–C bonds of the corannulene skeleton had been cleaved, and that the resulting vinyl group had been hydrogenated to form an ethyl group (Figure 2c). This presumption was also supported by electrospray ionization time-of-flight (ESI-TOF) mass spectrometry ( $m/z = 332.14$  for  $[\mathbf{2} + \text{H}]^+$ ).

The molecular structure of **2** was determined by single-crystal X-ray diffraction (XRD). As expected, the corannulene skeleton had been cleaved, and a benzo[ghi]fluoranthene skeleton bearing one ethyl group at the 6-position had been generated instead (Figure 3a). The resulting benzo[ghi]fluoranthene skeleton<sup>[12]</sup> is flat, which is in contrast to the curved structure of the corannulene skeleton of **1** with a bowl depth of 0.89 Å.<sup>[11]</sup> The flat moieties of **2** form a column through slipped  $\pi$ – $\pi$  stacking of the benzo[ghi]fluoranthene skeletons in the crystal structure (Figure 3b). This is in sharp contrast with the crystal packing of **1**, where no  $\pi$ – $\pi$  stacking of the curved corannulene skeletons was observed.<sup>[11]</sup>

We next focused on the mechanism of this reaction, which entails the cleavage of an aromatic C–C bond and subsequent reduction of the resulting vinyl group. To evaluate the mechanism, we conducted several control experiments using

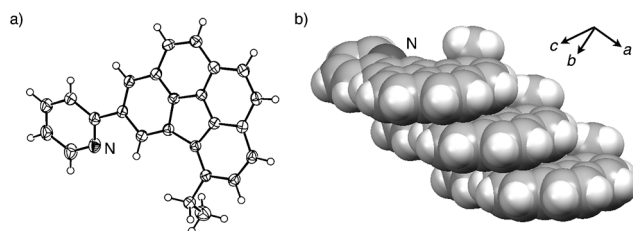


**Figure 3.** Crystal structure of **2**.<sup>[18]</sup> a) ORTEP view with the thermal ellipsoids set at 50% probability. b) The slipped  $\pi$ – $\pi$  stacking arrangement of **2**.

fragment compounds of **1** (Figure 4). For example, unsubstituted corannulene (**3**) did not react at all with  $\text{IrCl}_3 \cdot n\text{H}_2\text{O}$  at 250 °C in ethylene glycol under microwave irradiation. This indicates that the pyridine moiety is essential for this reaction. Furthermore, the simple addition of pyridine as a reagent to a reaction mixture with **3** did not facilitate the carbon–carbon bond scission reaction at all, suggesting that the 2-pyridyl group was required to be a substituent on the substrate.

We also examined a series of other fragment compounds possessing a smaller  $\pi$ -plane than **1**, namely 2-(naphthalen-1-yl)pyridine (**4**), 2-(phenanthren-9-yl)pyridine (**5**), and 2-(fluoranthren-3-yl)pyridine (**6**; Figure 4). In spite of the presence of

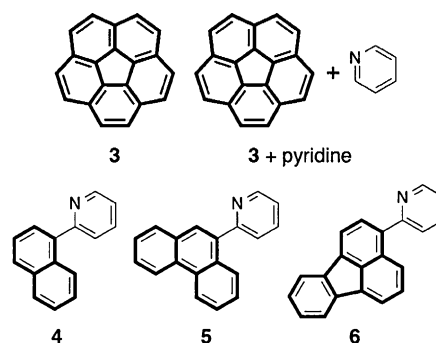


**Figure 4.** Fragment compounds of **1**. None of them gave any products that arise from a C–C bond cleavage reaction.

the 2-pyridyl substituent, no C–C bond cleavage reactions occurred in all cases, and the starting materials were recovered. Therefore, the non-planar structure of the corannulene skeleton should be another key factor facilitating the C–C cleavage reaction. In other words, this reaction is specific to 2-pyridylcorannulene (**1**), which comprises both the 2-pyridyl substituent and the curved corannulene skeleton.

Based on this finding, we propose a preliminary mechanism for this reaction (Figure 5). First, the starting iridium salt,  $\text{IrCl}_3 \cdot n\text{H}_2\text{O}$ , is reduced to a lower-valent iridium species,  $\text{Ir}^0$  or  $\text{Ir}^{\text{I}}$ , which then inserts into the aromatic C–C bond of the corannulene skeleton of **1** to form intermediate **I**, which features five- and seven-membered metallacycles with an  $\text{Ir}^{\text{II}}$  or  $\text{Ir}^{\text{III}}$  atom in association with its binding to the pendant 2-pyridyl group. After the oxidative addition, reduction of the resulting vinyl moiety and protonation afford product **2** and an  $\text{Ir}^{\text{II}}$  or  $\text{Ir}^{\text{III}}$  species. Although other intermediates, such as cyclometalated  $\text{Ir}^{\text{III}}$  complexes or olefin complexes, may be involved before or after the formation of **I**, we focus only on the key steps of the proposed mechanism to simply explain the site-selective C–C cleavage reaction of **1**.

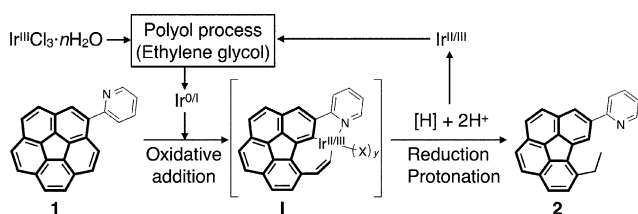


**Figure 5.** Plausible mechanism of the iridium-catalyzed reductive C–C bond cleavage reaction of **1**. X = solvents,  $\text{Cl}^-$ , and/or hydrides,  $y = 1–3$ .

The first step of this reaction, the reduction of  $\text{IrCl}_3 \cdot n\text{H}_2\text{O}$ , was experimentally confirmed by X-ray photoelectron spectroscopy (XPS). When we analyzed black solid samples obtained by microwave heating of  $\text{IrCl}_3 \cdot n\text{H}_2\text{O}$  in ethylene glycol at  $250^\circ\text{C}$  for five minutes, two distinct peaks corresponding to  $\text{Ir } 4f_{7/2}$  and  $\text{Ir } 4f_{5/2}$  were observed at 61.4 and 64.4 eV, respectively. These binding energies were significantly lower than those of  $\text{Ir}^{\text{III}}\text{Cl}_3$  (62.7 and 65.6 eV), suggesting that the  $\text{Ir}^{\text{III}}\text{Cl}_3$  salt was reduced to a lower-valent iridium species (Supporting Information, Figure S19). The disappearance of the peaks that are due to the Cl atoms also supports the reduction of  $\text{Ir}^{\text{III}}\text{Cl}_3$ . The binding energies of the reduced Ir components are close to those of metallic iridium,  $\text{Ir}^0$  (61.35 and 64.35 eV),<sup>[13]</sup> indicating that the resulting iridium species should be based on  $\text{Ir}^0$  or  $\text{Ir}^{\text{I}}$ . Indeed, these reaction conditions are very similar to those of a known method, the so-called polyol process, where metallic nanoparticles are produced from a transition-metal salt by heating in ethylene glycol at high temperature.<sup>[14]</sup> According to the literature, ethylene glycol reacts with a metal salt to afford elemental metal, 2,3-butanedione, and  $\text{HCl}$ .<sup>[14d]</sup> As iridium nanoparticles are also synthesized by a similar process,<sup>[14e]</sup> the formation of  $\text{Ir}^0$  species is likely to occur under these conditions.

As electron-rich transition metals in low oxidation states generally prefer to insert into C–C bonds through oxidative addition,<sup>[8a]</sup> we propose that the resulting low-valent iridium species,  $\text{Ir}^0$  or  $\text{Ir}^{\text{I}}$ ,<sup>[15]</sup> inserted into the aromatic C–C bond of the corannulene skeleton of **1** to form intermediate **I** with an  $\text{Ir}^{\text{II}}$  or  $\text{Ir}^{\text{III}}$  center (Figure 5). This mechanism is well supported by a recent theoretical study, in which metal insertion into a C–C bond at the edge of a carbon nanotube was proposed as the first step of the transition-metal-catalyzed unzipping of carbon nanotubes.<sup>[3]</sup> Furthermore, the proposed structure of intermediate **I** also meets several conditions that need to be fulfilled for C–C bond activation to occur, such as relieving strain energy, inducing aromatic stabilization, forming stable metallacyclic complexes, and chelation-assisted activation.<sup>[8a]</sup> For instance, intermediate **I** comprises two metallacycles, one of which is stabilized by chelation with the 2-pyridyl substituent. In fact, the 2-pyridyl moieties often serve as chelating auxiliaries in transition-metal-mediated C–H and C–C bond activation reactions.<sup>[16]</sup>

By the formation of intermediate **I**, the curved  $\pi$ -system of the corannulene skeleton of **1** is likely to be flattened to some extent through the iridium insertion because the planar benzo[ghi]fluoranthene skeleton of **I** is only loosely tethered

with a seven-membered metallacycle. Therefore, the relief of the nonplanar strain of the curved corannulene skeleton should be another key driving force for the formation of intermediate **I**. In the same way, more curved compounds (with a deeper cavity), such as a half fullerene ( $\text{C}_{30}\text{H}_{12}$ ) and open-cage fullerenes, are known to undergo C–C bond activation through oxidative addition,<sup>[9]</sup> and their nonplanar strain energy is much higher than that of corannulene according to a recent calculation.<sup>[10]</sup> Our observation of aromatic C–C bond cleavage in a carbon nanomaterial with a shallower curvature, namely corannulene, thus constitutes a rare example.<sup>[7]</sup>

The final step in the proposed mechanism entails reduction of the vinyl moiety and protonation to give product **2**. It was experimentally confirmed that our reaction conditions allowed for the hydrogenation of styrene to form ethylbenzene, even though the conversion was only approximately 50 % (Table S1). Accordingly, the possibility of direct hydride insertion from the iridium center to the metalated vinyl group cannot be excluded. The following protonation is likely to take place because  $\text{HCl}$  should be generated according to the mechanism of the polyol process. Consequently, the released iridium species with a higher oxidation state,  $\text{Ir}^{\text{II}}$  or  $\text{Ir}^{\text{III}}$ , should again be reduced by the polyol process to enter the catalytic cycle once again. Another possible pathway, the reductive elimination of  $\text{Ir}^{\text{II}}$  or  $\text{Ir}^{\text{III}}$  from a hydride complex and subsequent dissociation of  $\text{Ir}^0$  or  $\text{Ir}^{\text{I}}$ , might also be involved.

Finally, we investigated the metal specificity of this reaction by conducting screening experiments with various transition-metal chlorides ( $\text{FeCl}_3$ ,  $\text{CoCl}_2 \cdot 6\text{H}_2\text{O}$ ,  $\text{NiCl}_2 \cdot 6\text{H}_2\text{O}$ ,  $\text{CuCl}_2 \cdot 2\text{H}_2\text{O}$ ,  $\text{RuCl}_3$ ,  $\text{RhCl}_3 \cdot 3\text{H}_2\text{O}$ ,  $\text{PdCl}_2$ ,  $\text{AgCl}$ ,  $\text{IrCl}_3 \cdot n\text{H}_2\text{O}$ ,  $\text{PtCl}_2$ , and  $\text{Na}[\text{AuCl}_4] \cdot 2\text{H}_2\text{O}$ ) under almost identical conditions (with ca. 1 equiv or an excess amount of the metal salts). Interestingly, it was found that only  $\text{IrCl}_3 \cdot n\text{H}_2\text{O}$  provided full conversion of **1** into **2**. Other metal salts (except for  $\text{RuCl}_3$ , which afforded a rather complicated mixture including **1** and **2**) did not react with **1** at all, and the starting material was fully recovered after the reaction (Figures S23–S33). These results strongly indicate that the aromatic C–C bond cleavage reaction of **1** is specific to  $\text{IrCl}_3 \cdot n\text{H}_2\text{O}$  among the late transition metal chlorides that we tested, which is consistent with recent progress in C–C and C–H bond activation with Group 9 metals (Rh, Ir). The superiority of Ir over Rh has been reported for some C–C activation processes and was explained in terms of the stability of the M–C bonds.<sup>[8c]</sup>

In summary, we have demonstrated the efficient and site-selective C–C cleavage reaction of the corannulene skeleton of **1** by using  $\text{IrCl}_3 \cdot n\text{H}_2\text{O}$  and ethylene glycol as catalyst and solvent, respectively, with the aid of microwave heating at  $250^\circ\text{C}$ .<sup>[17]</sup> Several control experiments suggest that an Ir species obtained by in situ reduction reacted with **1** to form intermediate **I** in a process that is driven by both 2-pyridyl chelation and the relief of the nonplanar strain in the corannulene. Although several C–H and C–C bond activation reactions have been developed to date by means of elaborate iridium catalysts, the commercially available iridium salt  $\text{IrCl}_3 \cdot n\text{H}_2\text{O}$  used here is one of the simplest iridium catalysts. We envision that a further expansion of this reaction



will enabled the development of unique and efficient methods for the chemical modification of non-planar carbon nano-materials.

**Keywords:** annulenes · C–C activation · cleavage reactions · iridium · reaction mechanisms

**How to cite:** *Angew. Chem. Int. Ed.* **2015**, *54*, 5351–5354  
*Angew. Chem.* **2015**, *127*, 5441–5444

- [1] a) B. C. Thompson, J. M. J. Fréchet, *Angew. Chem. Int. Ed.* **2008**, *47*, 58–77; *Angew. Chem.* **2008**, *120*, 62–82; b) D. Tasis, N. Tagmatarchis, A. Bianco, M. Prato, *Chem. Rev.* **2006**, *106*, 1105–1136; c) A. K. Geim, K. S. Novoselov, *Nat. Mater.* **2007**, *6*, 183–191; d) H. Omachi, Y. Segawa, K. Itami, *Acc. Chem. Res.* **2012**, *45*, 1378–1389; e) Y.-T. Wu, J. S. Siegel, *Chem. Rev.* **2006**, *106*, 4843–4867.
- [2] a) F. Diederich, C. Thilgen, *Science* **1996**, *271*, 317–323; b) E. Nakamura, H. Isobe, *Acc. Chem. Res.* **2003**, *36*, 807–815; c) A. Hirsch, *Angew. Chem. Int. Ed.* **2002**, *41*, 1853–1859; *Angew. Chem.* **2002**, *114*, 1933–1939; d) S. Banerjee, T. Hemraj-Benny, S. S. Wong, *Adv. Mater.* **2005**, *17*, 17–29; e) V. Georgakilas, M. Otyepka, A. B. Bourlinos, V. Chandra, N. Kim, K. C. Kemp, P. Hobza, R. Zboril, K. S. Kim, *Chem. Rev.* **2012**, *112*, 6156–6214.
- [3] a) Y. Rubin, *Chem. Eur. J.* **1997**, *3*, 1009–1016; b) G. C. Vougioukalakis, M. M. Roubelakis, M. Orfanopoulos, *Chem. Soc. Rev.* **2010**, *39*, 817–844; c) K. Komatsu, M. Murata, Y. Murata, *Science* **2005**, *307*, 238–240; d) M. Terrones, *ACS Nano* **2010**, *4*, 1775–1781; e) P. M. Ajayan, T. W. Ebbesen, T. Ichihashi, S. Iijima, K. Tanigaki, H. Hiura, *Nature* **1993**, *362*, 522–525; f) J. Liu, A. G. Rinzier, H. Dai, J. H. Hafner, R. K. Bradley, P. J. Boul, A. Lu, T. Iverson, K. Shelimov, C. B. Huffman, F. Rodriguez-Macias, Y.-S. Shon, T. R. Lee, D. T. Colbert, R. E. Smalley, *Science* **1998**, *280*, 1253–1256; g) D. V. Kosynkin, A. L. Higginbotham, A. Sinitskii, J. R. Lomeda, A. Dimiev, B. K. Price, J. M. Tour, *Nature* **2009**, *458*, 872–876; h) J.-L. Li, K. N. Kudin, M. J. McAllister, R. K. Prud'homme, I. A. Aksay, R. Car, *Phys. Rev. Lett.* **2006**, *96*, 176101; i) Z. Li, W. Zhang, Y. Luo, J. Yang, J. G. Hou, *J. Am. Chem. Soc.* **2009**, *131*, 6320–6321; j) J. Wang, L. Ma, Q. Yuan, L. Zhu, F. Ding, *Angew. Chem. Int. Ed.* **2011**, *50*, 8041–8045; *Angew. Chem.* **2011**, *123*, 8191–8195.
- [4] a) W. E. Barth, R. G. Lawton, *J. Am. Chem. Soc.* **1966**, *88*, 380–381; b) H. Sakurai, T. Daiko, T. Hirao, *Science* **2003**, *301*, 1878.
- [5] a) L. T. Scott, M. M. Hashemi, M. S. Bratcher, *J. Am. Chem. Soc.* **1992**, *114*, 1920–1921; b) M. Juriček, N. L. Strutt, J. C. Barnes, A. M. Butterfield, E. J. Dale, K. K. Baldrige, J. F. Stoddart, J. S. Siegel, *Nat. Chem.* **2014**, *6*, 222–228; c) A. Sygula, F. R. Fronczek, R. Sygula, P. W. Rabideau, M. M. Olmstead, *J. Am. Chem. Soc.* **2007**, *129*, 3842–3843; d) W. Xiao, D. Passerone, P. Ruffieux, K. Ait-Mansour, O. Gröning, E. Tosatti, J. S. Siegel, R. Fasel, *J. Am. Chem. Soc.* **2008**, *130*, 4767–4771; e) M. A. Petrukhina, *Angew. Chem. Int. Ed.* **2008**, *47*, 1550–1552; *Angew. Chem.* **2008**, *120*, 1572–1574; f) A. V. Zabula, A. S. Filatov, S. N. Spisak, A. Y. Rogachev, M. A. Petrukhina, *Science* **2011**, *333*, 1008–1011; g) D. Miyajima, K. Tashiro, F. Araoka, H. Takezoe, J. Kim, K. Kato, M. Takata, T. Aida, *J. Am. Chem. Soc.* **2009**, *131*, 44–45; h) B. M. Schmidt, B. Topolinski, M. Yamada, S. Higashibayashi, M. Shionoya, H. Sakurai, D. Lentz, *Chem. Eur. J.* **2013**, *19*, 13872–13880.
- [6] a) E. A. Jackson, B. D. Steinberg, M. Bancu, A. Wakamiya, L. T. Scott, *J. Am. Chem. Soc.* **2007**, *129*, 484–485; b) A. Ueda, S. Nishida, K. Fukui, T. Ise, D. Shiomi, K. Sato, T. Takui, K. Nakasui, Y. Morita, *Angew. Chem. Int. Ed.* **2010**, *49*, 1678–1682; *Angew. Chem.* **2010**, *122*, 1722–1726; c) L. T. Scott, E. A. Jackson, Q. Zhang, B. D. Steinberg, M. Bancu, B. Li, *J. Am. Chem. Soc.* **2012**, *134*, 107–110; d) K. Kawasumi, Q. Zhang, Y. Segawa, L. T. Scott, K. Itami, *Nat. Chem.* **2013**, *5*, 739–744; e) B. Topolinski, B. M. Schmidt, M. Kathan, S. I. Troyanov, D. Lentz, *Chem. Commun.* **2012**, *48*, 6298–6300; f) B. M. Schmidt, D. Lentz, *Chem. Lett.* **2014**, *43*, 171–177.
- [7] a) X. Wang, H. Becker, A. C. Hopkinson, R. E. March, L. T. Scott, D. K. Böhme, *Int. J. Mass Spectrom. Ion Processes* **1997**, *161*, 69–76; b) S. Attar, D. M. Forkey, M. M. Olmstead, A. L. Balch, *Chem. Commun.* **1998**, 1255–1256; c) T. Hayama, Y.-T. Wu, A. Linden, K. K. Baldrige, J. S. Siegel, *J. Am. Chem. Soc.* **2007**, *129*, 12612–12613; d) Y. Inada, T. Amaya, Y. Shimizu, A. Saeki, T. Otsuka, R. Tsuji, S. Seki, T. Hirao, *Chem. Asian J.* **2013**, *8*, 2569–2574; e) X. Li, Y. Zhu, J. Shao, L. Chen, S. Zhao, B. Wang, S. Zhang, Y. Shao, H.-L. Zhang, X. Shao, *Angew. Chem. Int. Ed.* **2015**, *54*, 267–271; *Angew. Chem.* **2015**, *127*, 269–273.
- [8] a) K. Ruhland, *Eur. J. Org. Chem.* **2012**, 2683–2706; b) M. Murakami, T. Matsuda, *Chem. Commun.* **2011**, 47, 1100–1105; c) K. Ruhland, E. Herdtweck, *Adv. Synth. Catal.* **2005**, *347*, 398–404; d) C.-H. Jun, *Chem. Soc. Rev.* **2004**, *33*, 610–618; e) B. Rybtchinski, D. Milstein, *Angew. Chem. Int. Ed.* **1999**, *38*, 870–883; *Angew. Chem.* **1999**, *111*, 918–932; f) R. H. Crabtree, *Chem. Rev.* **1985**, *85*, 245–269; g) C. Perthuisot, B. L. Edelbach, D. L. Zubris, N. Simhai, C. N. Iverson, C. Müller, T. Satoh, W. D. Jones, *J. Mol. Catal. A* **2002**, *189*, 157–168; h) H. Schwager, S. Spyroudis, K. P. C. Vollhardt, *J. Organomet. Chem.* **1990**, *382*, 191–200.
- [9] a) R. M. Shaltout, R. Sygula, A. Sygula, F. R. Fronczek, G. G. Stanley, P. W. Rabideau, *J. Am. Chem. Soc.* **1998**, *120*, 835–836; b) F. Nunzi, A. Sgamellotti, N. Re, *Organometallics* **2002**, *21*, 2219–2225; c) M.-J. Arce, A. L. Viado, Y.-Z. An, S. I. Khan, Y. Rubin, *J. Am. Chem. Soc.* **1996**, *118*, 3775–3776; d) C.-S. Chen, Y.-F. Lin, W.-Y. Yeh, *Chem. Eur. J.* **2014**, *20*, 936–940.
- [10] C. H. Sun, G. Q. Lu, H. M. Cheng, *J. Phys. Chem. B* **2006**, *110*, 4563–4568.
- [11] M. Yamada, S. Tashiro, R. Miyake, M. Shionoya, *Dalton Trans.* **2013**, *42*, 3300–3303.
- [12] H. W. Ehrlich, C. A. Beevers, *Acta Crystallogr.* **1956**, *9*, 602–606.
- [13] M. A. Montero, J. L. Fernández, M. R. G. de Chialvo, A. C. Chialvo, *J. Phys. Chem. C* **2013**, *117*, 25269–25275.
- [14] a) F. Fiévet, J. P. Lagier, M. Figlarz, *MRS Bull.* **1989**, *14*, 29–34; b) F. Fiévet, J. P. Lagier, B. Blin, B. Beaudoin, M. Figlarz, *Solid State Ionics* **1989**, *32/33*, 198–205; c) S. Komarneni, R. Pidugu, Q. H. Li, R. Roy, *J. Mater. Res.* **1995**, *10*, 1687–1692; d) *Metal Nanoclusters in Catalysis and Materials Science: The Issue of Size Control* (Eds.: B. Corain, G. Schmid, N. Toshima), Elsevier, Netherlands, **2008**; e) F. Bonet, V. Delmas, S. Grugeon, R. H. Urbina, P.-Y. Silvert, K. Tekaia-Elhsissen, *Nanostruct. Mater.* **1999**, *11*, 1277–1284.
- [15] When we used Ir<sup>0</sup> black as the catalyst for the reaction of **1**, no reaction took place. This result may indicate that an Ir<sup>I</sup> species is involved in the oxidative addition reaction, but the possibility that the catalytic activity of Ir<sup>0</sup> black used here is much lower than that of in situ formed Ir<sup>0</sup> cannot be excluded.
- [16] a) Y. J. Park, J.-W. Park, C.-H. Jun, *Acc. Chem. Res.* **2008**, *41*, 222–234; b) H. Yorimitsu, K. Oshima, *Bull. Chem. Soc. Jpn.* **2009**, *82*, 778–792; c) D. A. Colby, R. G. Bergman, J. A. Ellman, *Chem. Rev.* **2010**, *110*, 624–655.
- [17] This reaction was very slow at 200°C; see the Supporting Information.
- [18] CCDC 1042770 (**2**) contains the supplementary crystallographic data for this paper. These data can be obtained free of charge from The Cambridge Crystallographic Data Centre via [www.ccdc.cam.ac.uk/data\\_request/cif](http://www.ccdc.cam.ac.uk/data_request/cif).

Received: January 28, 2015

Published online: March 10, 2015